ELSEVIER

Journal of Organometallic Chemistry 552 (1998) 177–186

Journal of Organometallic Chemistry

On the assignment of ^{119}Sn resonances of bis[dicarboxylatotetraorganodistannoxanes] in solution and solid state ^{119}Sn NMR spectra

François Ribot [a], Clément Sanchez [a], Abdelkrim Meddour [b], Marcel Gielen [c], Edward R.T. Tiekink [d], Monique Biesemans [b,c], Rudolph Willem [b,c,*]

[a] Laboratoire de Chimie de la Matière Condensée, URA CNRS 1466, Tour 54, 5e étage, Université Pierre et Marie Curie, 4 Place Jussieu, F-75252 Paris Cedex 05, France
[b] High Resolution NMR Centre (HNMR), Free University of Brussels (VUB), Pleinlaan 2, B-1050 Brussel, Belgium
[c] Laboratory of General and Organic Chemistry of the Faculty of Applied Sciences (AOSC), Free University of Brussels (VUB), Pleinlaan 2, B-1050 Brussel, Belgium
[d] Department of Chemistry, The University of Adelaide, Adelaide 5005, Australia

Received 2 July 1997

Abstract

The scope and limitations of ^{119}Sn resonance assignment strategies for structural characterizations of bis[dicarboxylatotetraorganodistannoxanes] by 2D gradient assisted ^{1}H–^{119}Sn HMQC NMR in solution and MAS ^{119}Sn NMR in the solid state are discussed for three compounds, the structure of which was already known by X-ray diffraction, bis[diacetatotetramethyldistannoxane] (**1**), bis[bis(2,2-dimethylpropanoato)tetramethyldistannoxane] (**3**), bis[bis(pentafluorobenzoato)tetra-*n*-butyldistannoxane] (**4**) and for the novel compound bis[bis(4-methylbenzoato)tetramethyldistannoxane] (**2**), for which an X-ray crystal structure is also reported. The structures of $\{R'COO(R_2Sn)–O–(SnR_2)OOCR'\}_2$ each feature a central $R_8Sn_4O_2$ core, and in addition to the μ_3-oxo links between the endo- and exo-cyclic tin atoms, the carboxylate ligands associating in a variety of structural motifs. Their relationship to ^{119}Sn MAS NMR patterns, in particular, the principal components of the ^{119}Sn shielding tensors, is discussed. © 1998 Elsevier Science S.A.

Keywords: ^{119}Sn resonances; Bis[dicarboxylatotetraorganodistannoxanes]; ^{119}Sn NMR spectra

1. Introduction

Bis[dicarboxylatotetraorganodistannoxanes], dimeric ladder structures obeying the formula $\{R'COO(R_2Sn)–O–(SnR_2)OOCR'\}_2$, are the subject of great interest, because of both their structural diversity in the crystalline state [1,2] and their interesting biological activity [3]. In principle, they are easily characterised in solution by standard NMR techniques, as their most common solution structure (Fig. 1, type A) gives rise to two equally intense ^{119}Sn resonances, appearing in the ^{119}Sn chemical shift range -170 to -230 ppm and exhibiting unresolved $^{2}J(^{119}Sn–O–^{119/117}Sn)$ coupling satellites [4–12].

The assignment of low and high frequency ^{119}Sn resonances to the exo (Sn2) and endo (Sn1) tin atoms of structure A is, however, conflicting in the literature [6,11,13,14]. Further, corresponding ^{119}Sn solid state NMR data on this type of compound are far from being well documented. This paper presents assignment investigations on the ^{119}Sn resonances, both in the solid and solution states, of four bis[dicarboxylatotetraorganodistannoxanes], $\{R'COO(R_2Sn)–O–(SnR_2)OOCR'\}_2$, bis[diacetato-tetramethyldistannoxane] (**1**; $R = CH_3$; $R' = CH_3$) [4], bis[bis(2,2-dimethyl-propanoato)tetramethyldistannoxane] (**3**; $R = CH_3$; $R' = C(CH_3)_3$) [13,14], bis[bis(pentafluoro-benzoato)tetra-*n*-butyldistannoxane] (**4**; $R = Bu$; $R' = C_6F_5$) [5], for which the X-ray struc-

---

[*] Corresponding author.

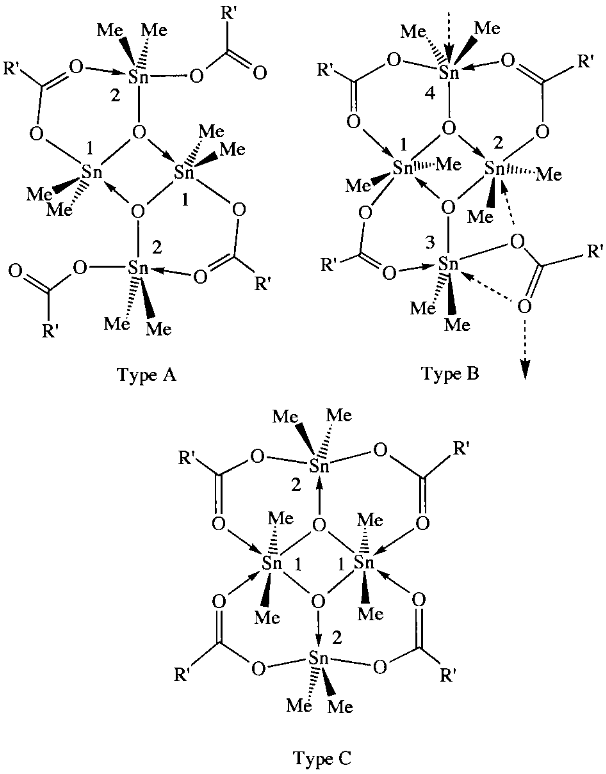

Fig. 1. Structures of dimeric bis[dicarboxylatotetramethyldistannoxanes]. The most usual solid-state structure, as well as the solution structure is of type A. In the case of **1**, the solid state structure is of type B and that of **3**, type C.

tures were already known, and for the compound bis[bis(4-methylbenzoato)tetramethyldistannoxane] (**2**; $R = CH_3$; $R' = p\text{-}CH_3\text{-}C_6H_4\text{–}$) [15], for which an X-ray structure is also reported.

2. Experimental

2.1. Syntheses

The compounds were prepared and characterised according to standard procedures described in the literature in Refs. [4,15] for **1**, [15] for **2**, [13,14] for **3** and [5] for **4**.

2.2. NMR experiments

The samples were prepared by dissolving ca. 40 mg of product in 0.5 ml of $CDCl_3$. All spectra were recorded at 303 K on a Bruker AMX500 spectrometer equipped with a digital lock and operating at 500.13, 125.77 and 186.50 MHz for ^1H, ^{13}C and ^{119}Sn nuclei respectively. Chemical shifts were referenced to the residual solvent peak ($CDCl_3$) and converted to the standard TMS scale by adding 7.23 ppm and 77.0 ppm for ^1H and ^{13}C nuclei, respectively. The ^{119}Sn reference frequency was calculated from the absolute frequency of Me_4Sn, which is 37.290 665 MHz [16–18] at the B_0 field corresponding to 100.000000 MHz for the ^1H nuclei in TMS.

Broad band ^1H-decoupled ^{13}C and ^{119}Sn spectra were recorded using the Bruker pulse sequences with standard delays. All heteronuclear correlation spectroscopy experiments consisted of gradient enhanced [19–22] versions of the standard HMQC [23] and HMBC [24,25] pulse sequences, all processed in the magnitude mode. In particular, the gradient enhanced [19–22] $^1H–^{119}Sn$ HMQC [26–28] and the $^1H–^{13}C$ HMBC [24,25] experiments have been implemented in exactly the same way as presented recently [29].

The ^{119}Sn MAS (Magic Angle Spinning) experiments [30,31] have been performed on a Bruker MSL300 spectrometer (111.89 MHz for ^{119}Sn) equipped with a 4 mm locked Bruker probe. The spectral width was 200 000 Hz ($\approx$ 1800 ppm). Pulse angles were about 30° (1.5 μs) and recycling delays 15 s. Typically 1000 to 5000 transients were recorded for each sample in order to achieve reasonable signal-to-noise ratios. Chemical shifts are quoted relative to Me_4Sn, using solid tetracyclohexyltin ($\delta_{iso} = -97.35$ ppm) as a secondary external reference [32]. At least two experiments, with sufficiently different spinning rates, were run in order to identify isotropic chemical shifts. The principal components of the ^{119}Sn shielding tensors were analysed with WINFIT software [33] using the Herzfeld and Berger approach [34]. They are reported, following Haeberlen's notation [35] as the isotropic chemical shift ($\delta_{iso} = -\sigma_{iso}$), the anisotropy ($\zeta = \sigma_{33} - \sigma_{iso}$) and the asymmetry ($\eta = |\sigma_{22} - \sigma_{11}|/|\sigma_{33} - \sigma_{iso}|$), σ_{11}, σ_{22} and σ_{33} being the three components of the shielding tensor expressed in its principal axis system with the following rule: $|\sigma_{33} - \sigma_{iso}| \geq |\sigma_{11} - \sigma_{iso}| \geq |\sigma_{22} - \sigma_{iso}|$. With this writing convention, ζ is a signed value expressed in ppm. The accuracy on δ_{iso}, ζ and η corresponds to ±0.5 ppm (digital resolution), ±10 ppm and ±0.05, respectively.

2.3. NMR characteristics

2.3.1. Compound 1 [15]

^1H NMR: CH_3–C 1.92, 12H; CH_3Sn1 0.81, s [$^2J(^1H–^{119/117}Sn) = 91/87$], 12H; CH_3Sn2 0.79, s [$^2J(^1H–^{119/117}Sn) = 87/83$], 12H. Lit. [4]: CH_3Sn1 0.79 [$^2J(^1H–^{119}Sn) = 89.0$]; CH_3Sn2 0.77 [$^2J(^1H–^{119}Sn) = 86.8$]. ^{13}C NMR: CH_3–C 22.9; CO 177.6; CH_3Sn1 8.7 [$^1J(^{13}C–^{119/117}Sn) = 802/768$]; CH_3Sn2 5.9 [$^1J(^{13}C–^{119/117}Sn) = 752/713$]. Lit. [4]: CH_3Sn1 5.9 [$^1J(^{13}C–^{119}Sn) = 748$]; CH_3Sn2 8.7 [$^1J(^{13}C–^{119}Sn) = 800$]. ^{119}Sn NMR: Sn1 −190.2 (broad; $^2J(^{119}Sn–^{119/117}Sn)$ unresolved); Sn2 −173.8 [$^2J(^{119}Sn–^{119/117}Sn) = 110$].

2.3.2. Compound **2** [15]

^{1}H NMR: CH_3–p 2.40, 12H; Ho 7.87, d [8], 8H; Hm 7.23, d [8], 8H; CH_3Sn1 0.99, s [$^2J(^1H–^{119}Sn)$ 92], 12H; CH_3Sn2 0.94, s [$^2J(^1H–^{119}Sn)$ 90], 12H. ^{13}C NMR: CH_3–p 21.7; CO 173.2; ipso 129.0; ortho 130.4; meta 129.9; para 142.8; CH_3Sn1 7.0 [$^1J(^{13}C–^{119/117}Sn) = 770/734$]; CH_3Sn2 10.0 [$^1J(^{13}C–^{119/117}Sn) = 818/783$]. ^{119}Sn NMR: Sn1 -190.1 (broad; $^2J(^{119}Sn–^{119/117}Sn)$ unresolved); Sn2 -179.4 [$^2J(^{119}Sn–^{119/117}Sn) = 101$].

2.3.3. Compound **3** [13,14]

^{1}H NMR: CH_3–C 1.13, 36H; CH_3Sn1 and CH_3Sn2 0.787, s [$^3J(^1H–^{119/117}Sn) = 92/88$], 12H; 0.724, s [$^2J(^1H–^{119/117}Sn) = 91/87$], 12H. Lit. [13]: CH_3Sn1 0.78, s [$^3J(^1H–^{119/117}Sn) = 90$], 12H, CH_3Sn2 0.72, s [$^2J(^1H–^{119/117}Sn) = 84$], 12H;. ^{13}C NMR: $\mathit{C}H_3$–C 27.6; $\mathit{C}H_3$–C 39.2; CO 186.0; CH_3Sn1 8.9 [$^1J(^{13}C–^{119/117}Sn) = 801/783$]; CH_3Sn2 6.9 [$^1J(^{13}C–^{119/117}Sn) = 799/762$]. Lit. [13]: $\mathit{C}H_3$–C 27.6; CH_3–C 39.1; CO 186.0; CH_3Sn1 8.8; CH_3Sn2 6.8. ^{119}Sn NMR: Sn1 -188.2 (broad; $^2J(^{119}Sn–^{119/117}Sn)$ unresolved); Sn2 -195.1 [$^2J(^{119}Sn–^{119/117}Sn) = 96$]. Lit. [13]: Sn1 and Sn2 -188 and -194.

2.3.4. Compound **4** [5]

Complete NMR data were described previously [5].

2.4. Crystallography for **2**

Colourless crystals of bis[bis(4-methylbenzoato)tetramethyldistannoxane] (**2**) were grown from dichloromethane/hexane 3/1 (v/v) [15]. Intensity data for a crystal ($0.13 \times 0.19 \times 0.26$ mm) were collected at room temperature on a Rigaku AFC6R employing MoKα radiation ($\lambda = 0.71073$ Å) and the ω:2θ scan technique. The 5568 unique data (θ_{max} 27.5°) were corrected for Lorentz and polarisation effects [36] as well as for absorption employing an empirical procedure [37]; the range of transmission factors was 0.562 to 1. A total of 3644 data satisfied the $I \geq 3.0\sigma(I)$ criterion of observability and were used in the subsequent analysis.

Crystal data for **2**: $C_{40}H_{52}O_{10}Sn_4$, $M = 1167.6$, monoclinic, space group $C2/c$, $a = 31.47(3)$, $b = 7.816(5)$, $c = 23.57(2)$ Å, $\beta = 129.08(5)°$, $V = 4500(7)$ Å^3, $Z = 4$, $D_{calc} = 1.723$ g cm^{-3}, $F(000) = 2288$, $\mu = 22.44$ cm^{-1}, $R = 0.038$, $R_w = 0.040$.

The structure was solved by direct methods [38] and refined by a full-matrix least-squares procedure based on F [36]. All non-hydrogen atoms were refined with anisotropic displacement parameters and hydrogen atoms were included in the model at their calculated positions (C–H 0.97 Å). The refinement was continued until convergence employing sigma weights, i.e., $1/\sigma^2(F)$, when $R = 0.038$ and $R_w = 0.040$. The maximum peak in the final difference map was 0.72 e Å^{-3} and the analysis of variance showed no special features. Fractional atomic coordinates are listed in Table 1, selected interatomic parameters are collected in Table 2 and the crystallographic numbering scheme for the molecule is shown in Fig. 4; drawn with ORTEP [39] at 35% probability ellipsoids. A copy of the CIF and the observed and calculated structure factors are available from E.R.T.T. (etiekink@chemistry.adelaide.edu.au).

3. Results and discussion

3.1. Basic solution ^{119}Sn NMR assignments

The ^{119}Sn NMR spectrum of **1** in $CDCl_3$ solution reveals two equally intense ^{119}Sn resonances at -173.8 and -190.2 ppm, with the latter being broad, in good agreement with literature data (-174.4 and -190.0 ppm) [11]. These solution chemical shifts clearly favour the type A structure (Fig. 1) in which both the endocyclic (Sn1) and exocyclic (Sn2) tin atoms are five-coordinate and display trigonal bipyramidal geometry rather than six-coordination [1,2,5–11,18]. This structure is known to be the most common one, in both solid and solution states [1,2,5–11,13,14,40]. The $^1J(^{13}C–^{119}Sn)$ coupling constants of 752 and 802 Hz, corresponding to angles [41] of respectively, 142 and 147°

Table 1
Fractional atomic coordinates for non-hydrogen atoms in **2**

Atom	x	y	z
Sn(1)	0.06349(2)	−0.04020(5)	0.57103(2)
Sn(2)	0.02820(2)	0.00342(5)	0.38595(2)
O(1)	0.0156(1)	−0.0023(5)	0.4605(2)
O(2)	0.1341(2)	−0.0989(6)	0.5730(2)
O(3)	0.1194(2)	0.0293(6)	0.4787(2)
O(4)	−0.0610(2)	0.0217(5)	0.3176(2)
O(5)	−0.0621(2)	−0.0303(7)	0.2248(2)
C(1)	0.1505(3)	−0.0264(8)	0.5434(3)
C(2)	0.2112(2)	−0.0071(7)	0.5867(3)
C(3)	0.2330(3)	0.0642(8)	0.5561(3)
C(4)	0.2888(2)	0.0763(8)	0.5960(3)
C(5)	0.3251(2)	0.0186(8)	0.6680(4)
C(6)	0.3862(3)	0.026(1)	0.7101(4)
C(7)	0.3024(2)	−0.0497(9)	0.6978(3)
C(8)	0.2469(2)	−0.0630(8)	0.6584(3)
C(9)	−0.0863(2)	−0.0037(8)	0.2478(3)
C(10)	−0.1486(2)	−0.0024(7)	0.1987(3)
C(11)	−0.1776(3)	−0.0711(8)	0.1294(3)
C(12)	−0.2344(2)	−0.0746(8)	0.0824(3)
C(13)	−0.2633(2)	−0.0034(8)	0.1039(3)
C(14)	−0.3248(3)	0.001(1)	0.0511(4)
C(15)	−0.2332(2)	0.0655(9)	0.1732(4)
C(16)	−0.1772(2)	0.0669(9)	0.2198(3)
C(17)	0.0363(3)	0.2523(9)	0.3600(3)
C(18)	0.0364(3)	−0.2538(9)	0.3685(4)
C(19)	0.0661(3)	−0.3036(9)	0.5907(3)
C(20)	0.0992(3)	0.2019(9)	0.6150(4)

Table 2
Selected bond distances (Å) and angles (deg.) for **2**[a]

Sn(1)–O(1)	2.049(4)	Sn(2)–O(1)	2.031(4)
Sn(1)–O(1)′	2.126(4)	Sn(2)–O(3)	2.269(4)
Sn(1)–O(2)	2.240(4)	Sn(2)–O(4)	2.190(4)
Sn(1)–C(19)	2.100(7)	Sn(2)–C(17)	2.102(7)
Sn(1)–C(20)	2.109(7)	Sn(2)–C(18)	2.100(7)
C(1)–O(2)	1.236(7)	C(9)–O(4)	1.316(7)
C(1)–O(3)	1.262(7)	C(9)–O(5)	1.201(7)
C(1)–C(2)	1.502(8)	C(9)–C(10)	1.523(8)
O(1)–Sn(1)–O(1)′	76.8(2)	O(1)–Sn(2)–O(3)	89.3(2)
O(1)–Sn(1)–O(2)	88.9(2)	O(1)–Sn(2)–O(4)	77.2(2)
O(1)–Sn(1)–C(19)	108.5(2)	O(1)–Sn(2)–C(17)	113.4(2)
O(1)–Sn(1)–C(20)	103.4(2)	O(1)–Sn(2)–C(18)	105.2(2)
O(1)′–Sn(1)–O(2)	165.0(1)	O(3)–Sn(2)–O(4)	163.6(2)
O(1)′–Sn(1)–C(19)	96.0(2)	O(3)–Sn(2)–C(17)	83.4(2)
O(1)′–Sn(1)–C(20)	100.1(2)	O(3)–Sn(2)–C(18)	92.1(2)
O(2)–Sn(1)–C(19)	83.9(2)	O(4)–Sn(2)–C(17)	93.5(2)
O(2)–Sn(1)–C(20)	87.7(2)	O(4)–Sn(2)–C(18)	100.2(2)
C(19)–Sn(1)–C(20)	146.8(3)	C(17)–Sn(2)–C(18)	141.0(3)
Sn(1)–O(1)–Sn(1)′	103.2(2)	Sn(1)–O(1)–Sn(2)	135.6(2)
Sn(1)–O(1)–Sn(2)′	121.2(2)	Sn(1)–O(2)–C(1)	131.0(4)
Sn(2)–O(3)–C(1)	132.8(4)	Sn(2)–O(4)–C(9)	113.2(4)
O(2)–C(1)–O(3)	124.0(6)	O(4)–C(9)–O(5)	122.4(6)

[a] Primed atoms related by the symmetry relation: $-x$, $-y$, $1-z$.

for the exocyclic and endocyclic tin atoms, are in agreement with this.

As no decisive ^{119}Sn chemical shift argument can be invoked, a 2D gradient assisted [19–22] ^{1}H–^{119}Sn [26–28] HMQC [23] experiment was necessary to make an unambiguous assignment of the ^{119}Sn resonances to the endo (Sn1) and exo (Sn2) tin atoms possible.

Fig. 2 shows the two pairs of $^{2}J(^{1}\text{H}–^{119}\text{Sn})$ cross-peak satellites expected in the 2D ^{1}H–^{119}Sn HMQC spectrum of **1** between its methyl protons and its ^{119}Sn nuclei, two cross-peaks A and B associated with the low frequency ^{119}Sn resonance and a single cross-peak C associated with the high frequency one. The cross-peaks A, B and C are assigned to unresolved pairs of $^{4}J(^{1}\text{H}–^{119}\text{Sn})$ cross-peak satellites. If it is assumed, reasonably, that the long range $^{6}J(^{1}\text{H}–^{119}\text{Sn})$ coupling between CH_3Sn2 and Sn2′ is invisible under the acquisition conditions used (delay of 250 ms), the assignment of the low frequency ^{119}Sn resonance (−190.2 ppm) to the endo tin atom Sn1 is straightforward, since the ^{119}Sn resonance of the exo tin atoms Sn2/Sn2′ can exhibit only a single $^{4}J(^{1}\text{H}–^{119}\text{Sn})$ correlation, the (double) coupling pathway ^{1}H–C–Sn1/Sn1′–O–^{119}Sn2 generating cross-peak C. By contrast, the endo tin atoms Sn1/Sn1′ can exhibit two $^{4}J(^{1}\text{H}–^{119}\text{Sn})$ correlations, the (double) coupling pathway ^{1}H–C–Sn2/Sn2′–O–^{119}Sn1 generating cross-peak B, and the (single) coupling pathway ^{1}H–C–Sn1′–O–^{119}Sn1 generating cross-peak A. This completes simultaneously, the methyl proton assignment as given in Section 2, together with the associated ^{13}C resonance assignment achieved by a ^{1}H–^{13}C HMQC experiment.

A similar assignment is proposed for compound **2**, the ^{119}Sn chemical shifts (−179.4 and −190.1 ppm) being very similar to those of **1**, and the low frequency ^{119}Sn resonance being again broader. Further evidence by a ^{1}H–^{119}Sn HMQC experiment was not found for this because fast relaxation indicated by the globally higher line-width of the **2** ^{119}Sn resonances prevented the observation of long range ^{1}H–^{119}Sn correlations.

The high frequency ^{119}Sn signal around −175 ppm exhibits unresolved $^{2}J(^{119}\text{Sn–O–}^{119/117}\text{Sn})$ coupling satellites of 110 Hz for **1** (lit. [4]: 103 Hz) and of 101 Hz for **2**. By contrast, the large line-width of the low frequency ^{119}Sn resonance at −190 ppm makes such satellites invisible.

The ^{1}H and ^{13}C resonances of **2** have been assigned by 2D ^{1}H–^{13}C HMBC and HMQC experiments.

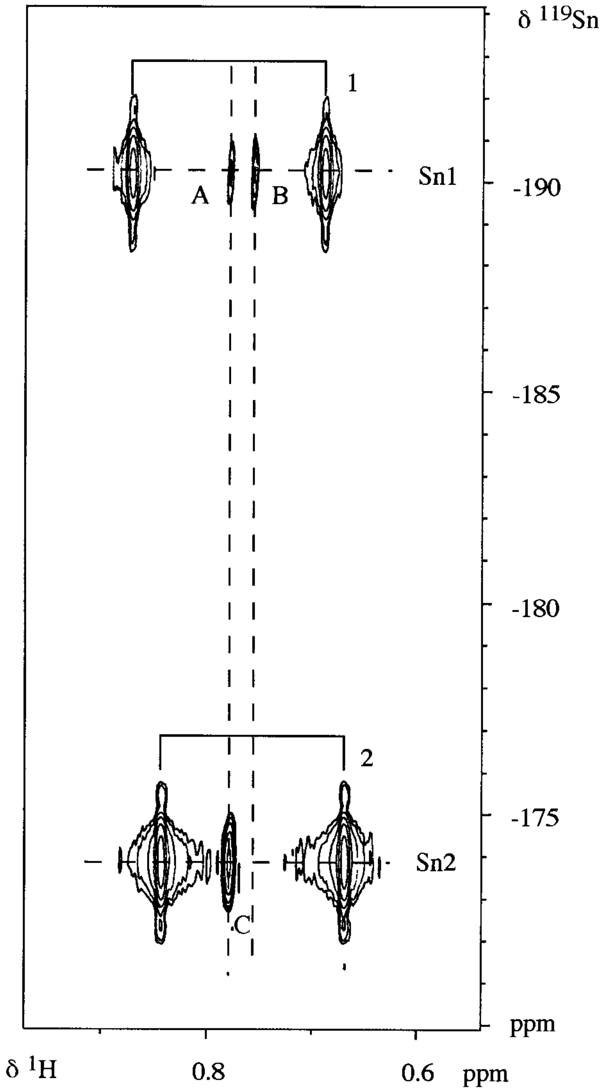

Fig. 2. 2D gradient assisted ^{1}H–^{119}Sn HMQC spectrum of compound **1**.

The solution chemical shifts of −188.2 and −195.1 ppm for **3**, $\{[Me_2Sn(O_2C\text{–}t\text{Bu})]_2O\}_2$, agree with literature data (−188 and −194 ppm [13]) and also favour a type A structure (Fig. 1) in solution. However, a 2D gradient assisted ^{1}H–^{119}Sn HMQC spectrum of **3** points towards an assignment opposite to the one made for **1** (Fig. 2) and **2**, since for **3**, the cross-peak C appears at the low frequency ^{119}Sn resonance while cross-peaks A and B, accordingly, appear at the high frequency ^{119}Sn resonance. The low and high frequency chemical shifts, −194.8 and −187.8 ppm, correspond therefore to the exo (Sn2) and endocyclic (Sn1) tin atoms, respectively. This assignment is further supported by the larger linewidth of the high frequency ^{119}Sn resonance in the solution ^{119}Sn NMR spectrum of **3**, in contrast with the broad resonance being at low frequency for **1** and **2**. This last point shows how small changes in the nature of the carboxylate ligand can modify the ^{119}Sn chemical shifts, and emphasises that no general rules can be formulated for the assignment of the ^{119}Sn resonances to the endo and exo tin atoms of bis[dicarboxylatotetraorganodistannoxanes] in solution.

3.2. ^{119}Sn MAS NMR assignments

Compounds **1**, **2** and **3** exhibit very close solution behaviour, yet **1** and **3** are known to adopt the uncommon structures of type B and C, respectively, in the solid state (Fig. 1) [1,4,13]. The ^{119}Sn MAS NMR spectra for compounds **1**, **2** and **3** were recorded in order to investigate whether ^{119}Sn MAS spectra can provide reliable predictive information on the solid state structure of such bis[dicarboxylatotetraorganodistannoxanes]. Given the lack of information on solid state ^{119}Sn NMR of bis[dicarboxylatotetraorganodistannoxanes], the ^{119}Sn MAS NMR spectrum of $\{[Bu_2Sn(O_2CC_6F_5)]_2O\}_2$ [5], compound **4**, the crystalline structure of which is known to be of type A (Fig. 1), was also recorded for comparative purposes. A common feature of all spectra is the appearance of a relatively large number (8 to 9) of spinning side bands for each tin site, despite the high spinning rates of 13 to 15 kHz used. In order to determine the relative populations of the tin sites and also to extract the principal components of the ^{119}Sn shielding tensors of the different tin sites, the spectra were iteratively adjusted assuming a pure chemical shift anisotropy (CSA) behaviour for tin [33,34]. The ^{119}Sn MAS NMR analysis results are reported in Table 3 and Fig. 3 shows the ^{119}Sn MAS NMR spectra of **1** and **2**, together with their simulations.

The number of tin sites determined by ^{119}Sn MAS NMR for compounds **1**, **3** and **4** confirms their non-equivalence in their respective X-ray diffraction structures: four equally populated for **1** [4], two pairwise equally populated for **3** [13] and **4** [5].

Assignment of the various solid state ^{119}Sn NMR resonances is not straightforward. Even though literature on solid state ^{119}Sn NMR is growing, a clear correlation, theoretical or empirical, between δ_{iso}, ζ, η (or σ_{11}, σ_{22}, σ_{33}) and structure is not yet achieved and will probably require a thorough compilation of experimental data [42]. Among the ^{119}Sn MAS NMR spectra of the three compounds of known structure (**1**, **3** and **4**), the one for **3** is probably the most straightforward to relate to the solid state structure. Compound **3**, in the solid state, exhibits a type C structure (Fig. 1) with two non-equivalent pairs of tin atoms [13,14]. The Sn–C distances are close to 2.10 Å and the Sn–O distances range from 2.00 to 2.35 Å. All the other Sn–O distances (intra or intermolecular) are longer than 3.20 Å and can be stated to have negligible contribution to the ^{119}Sn δ_{iso} value. Therefore, the endocyclic tin, Sn1, is six-coordinate, while the exocyclic tin, Sn2, is five-coordinate. Given the low frequency shift upon coordination increase for a given organotin moiety (mono-, di- or

Table 3
^{119}Sn MAS NMR data on compounds **1**–**4**

Compound	δ_{iso}^{a} (ppm)	ζ^{a} (ppm)	η^{a}	Rel. area[b] (%)	CN[c]	σ_{11}^{a} (ppm)	σ_{22}^{a} (ppm)	σ_{33}^{a} (ppm)	Assignment[d]
1	−178	617	0.60	26	5	−316	55	795	Sn2 or Sn3
	−209	603	0.80	24	5	−334	149	812	Sn3 or Sn2
	−287	657	0.30	24	6	−140	57	944	Sn4 (or Sn1)[e]
	−298	697	0.30	26	6	−155	54	995	Sn1 (or Sn4)[e]
2	−195	643	0.65	54	5	−335	82	838	Sn1 or Sn2
	−233	603	0.60	46	5	−249	112	836	Sn2 or Sn1
3	−184	576	0.85	48	5	−349	140	760	Sn2
	−267	644	0.40	52	6	−184	74	911	Sn1
4	−177	630	0.45	45	5	−280	4	807	Sn1 or Sn2
	−219	710	0.55	55	5	−331	59	929	Sn2 or Sn1

[a] $\delta_{iso} = -\sigma_{iso} = -(\sigma_{11}+\sigma_{22}+\sigma_{33})/3$; $\zeta = \sigma_{33}-\sigma_{iso}$; $\eta = |\sigma_{11}-\sigma_{22}|/\zeta$ $|\sigma_{33}-\sigma_{iso}| \geq |\sigma_{11}-\sigma_{iso}| \geq |\sigma_{22}-\sigma_{iso}|$.
[b] Including all the spinning side bands.
[c] CN = coordination number.
[d] See Fig. 1 for atom numbering.
[e] See text.

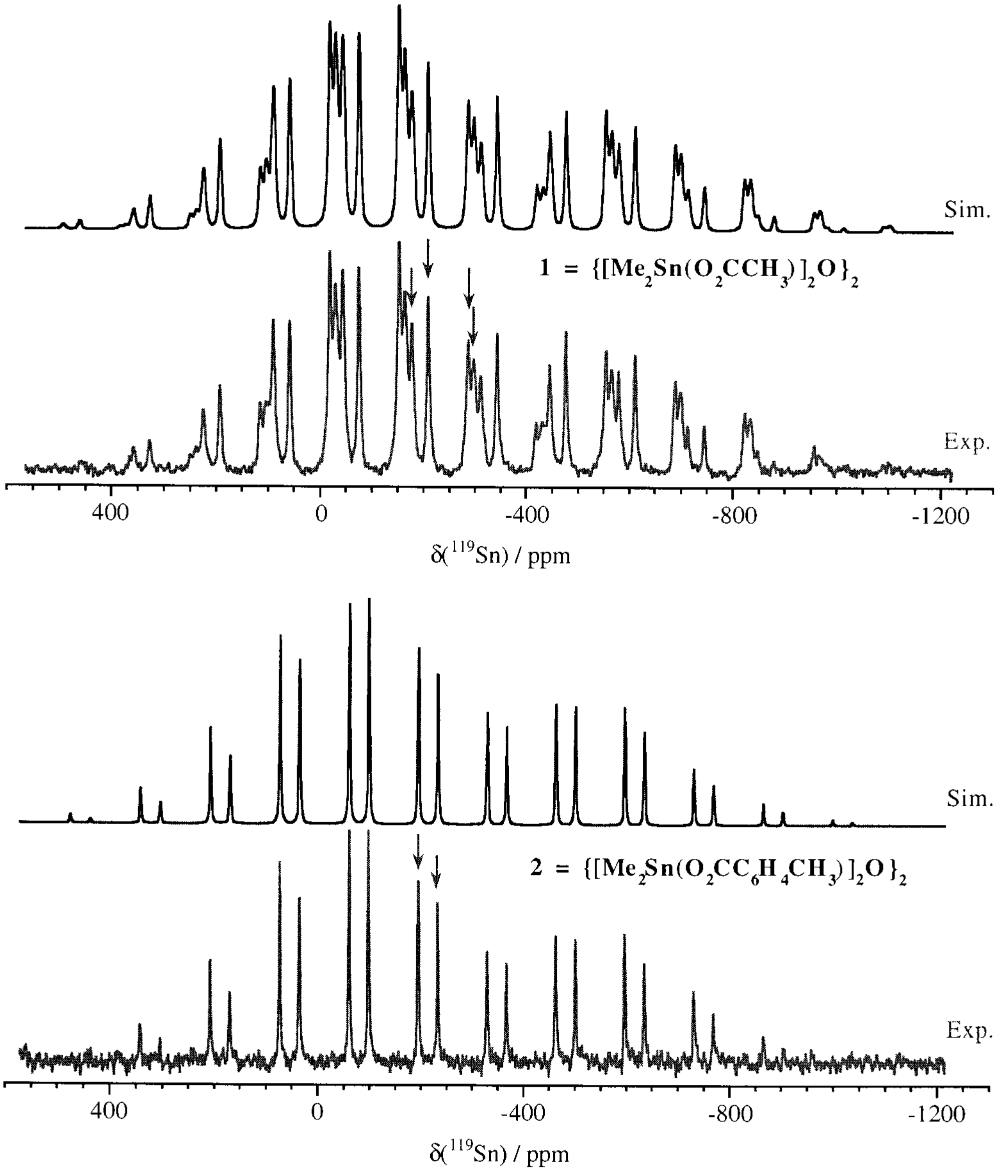

Fig. 3. ^{119}Sn MAS NMR spectra (ν_{MAS} = 15 000 Hz) and their simulations for compounds **1** and **2**. Isotropic chemical shifts are pointed with arrows.

tri-organotin), the −267 and −184 ppm isotropic chemical shifts can be, respectively, assigned to the endo and exocyclic tin atoms. The difference (83 ppm) is smaller than the usual value (around 150 ppm) for an increase of the coordination number by one unit [42,43], yet, it can be explained by the trapezoidal bipyramidal geometry of the endocyclic tin atoms, their equatorial plane containing two short Sn–O bonds, 2.110(5) and 2.088(5) Å, and two long Sn–O bonds, 2.353(7) and 2.330(7) Å [13]. Such a trapezoidal bipyramidal geometry [1,4,9,10,44–50] is known to be characterised by ^{119}Sn resonances shifted by 40 to 60 ppm to higher frequency than less distorted pseudo-octahedral environments [1,9,10,44–50].

Compound **1** displays a more complex structure (type B in Fig. 1) in the solid state, with four non-equivalent tin atoms [4]. Two, Sn1 and Sn4, are six-coordinate with distorted octahedral geometries (Me–Sn–Me angles are 158(1) and 157.5(9)° for Sn1 and Sn4, respectively [4]), while the two others, Sn2 and Sn3, can be considered as five-coordinate with distorted trigonal bipyramidal geometries (Me_2O equatorial plane), if Sn–O contacts longer than 2.80 Å are neglected [1]. According to the coordination rule presented above for **3**, the low frequency isotropic chemical shifts, −298 and −287 ppm, can be assigned to six-coordinate tin atoms while the high frequency ones, −209 and −178 ppm, to five-coordinate tin atoms. Both isotropic chemical shift domains, ca. -290 and -190 ppm, are similar to those of compound **3**. This point, especially for the high frequency domain, would confirm the relatively low effect of the fourth longer intramolecular Sn $\cdots$ O contacts, 2.89(1) and 2.92(1) Å for Sn2 and Sn3, respectively. Indeed, these longer contacts do not prevent the geometry of Sn2 and Sn3 to be basically five-coordinate as supported by their Me–Sn–Me angles of 143(1) and 139(1)° [4], more characteristic of a trigonal bipyramid (120°) than of an octahedron (180°).

Further analysis of the ^{119}Sn NMR assignment for **1** is speculative at this stage. It could be proposed that the isotropic chemical shift at -287 ppm, the one at high frequency among the two low frequency ones, arises from Sn4 which should be less shielded because one of its Sn–O bonds is definitely longer (2.56(1) Å, for the intermolecular contact [4]).

Compound **4**, which exhibits a type A structure (Fig. 1) in the solid state, contains two non-equivalent tin atoms which are basically five-coordinate with distorted trigonal bipyramidal geometries (C–Sn–C angles are 140.1(3) and 144.9(3)° for Sn1 and Sn2, respectively) [5]. The two ^{119}Sn isotropic chemical shifts observed for **4** (-177 and -219 ppm) are within the range for five-coordinate tin atoms, as already observed in **1** and **3**, even though the alkyl groups bound to tin are butyl groups in **4** rather than methyl ones in **1** to **3**. As for the five-coordinate Sn2/Sn3 tin atoms in **1**, fairly long fourth intramolecular Sn–O contacts are also present in **4** (2.869(4) and 2.829(5) Å for Sn1 and Sn2, respectively) [5], but they are obviously again of very little influence, as they were in **1**.

The above analysis indicates that using isotropic ^{119}Sn chemical shifts from MAS spectra should be done with extreme care whenever solid state structure types are to be proposed when no X-ray diffraction data are available for such distannoxanes. However, with ^{119}Sn chemical shifts of ca. -250 to -260 ppm or less, the onset to six-coordination can be delineated since the above analysis reveals little additional ^{119}Sn shielding for additional Sn $\cdots$ O contacts above 2.5 to 2.6 Å.

As previously noted, the relatively small amount of literature data dealing with the correlation between structure and principal components of the ^{119}Sn shielding tensors makes the discussion on the anisotropies (ζ) and asymmetries (η) determined for **1**, **3** and **4** (Table 3) almost impossible [42]. Moreover, it is usually not possible to find simple relations between the principal axis system of the shielding tensor and the molecular axis centred at the tin atoms [51]. Yet, with the assignments proposed on the basis of the isotropic chemical shifts, the following comments can be made for the shielding tensorial properties of **1**, **3** and **4**. Within a given compound, the anisotropies of six-coordinate tin atoms appear larger by 40 to 100 ppm than those of five-coordinate tin atoms. However, the highest value observed concerns one of the two five-coordinate tin atoms of compound **4** [5]. All the asymmetries appear to comply the following rule: they lie between 0.3 and 0.5 for six-coordinate tin atoms, while they are larger than 0.5, up to 0.8, for five-coordinate tin atoms. This can alternatively be expressed on the shielding principal components; thus, σ_{22} seems rather unpredictable, but σ_{33} and σ_{11} are more coordination related. Five-coordinate tin atoms are associated with σ_{33} and σ_{11} values around 790 (± 30) and -320 (± 40) ppm, respectively, at least, if the rather strange σ_{33} value observed for the low frequency resonance of **4**, which already exhibited the largest anisotropy, is excepted. By contrast, six-coordinate tin atoms give rise to σ_{33} and σ_{11} values around 950 (± 45) and -160 (± 25) ppm, respectively. It is worth mentioning that the changes of σ_{33} and σ_{11} with an increase of the coordination number by one unit match better the usually acknowledged 150 ppm shift [42,43].

3.3. X-ray data

From the comparative examination of literature X-ray data on compounds **1**, **3** and **4** and our ^{119}Sn MAS data, including not only the isotropic chemical shifts but also the principal components of the ^{119}Sn shielding tensors, the limit between actual six-coordination and five-coordination with an additional weak contact can be delineated. A pairwise accidental resonance isochrony being very unlikely, the ^{119}Sn MAS NMR spectrum of **2**, and the principal components of the ^{119}Sn shielding tensors extracted herefrom, indicate two equally populated five-coordinate tin sites ($\delta_{iso} = -195$ and -233 ppm) suggesting that its solid state structure is of structural type A (Fig. 1). In order to assess the predictive power of ^{119}Sn MAS data for the solid state structure determination of bis[dicarboxylatotetraorganodistannoxanes], the X-ray crystal structure of the novel compound **2** was likewise determined.

The molecular structure of **2** is shown in Fig. 4 and selected interatomic parameters are collected in Table 2. The structure indeed conforms to the common motif, i.e., type A, as shown in Fig. 1. The structure is centrosymmetric with both bidentate bridging and monodentate terminal carboxylate ligands. This arrangement gives rise to trigonal bipyramidal geometries about both the endo- and exo-cyclic tin atoms. The Sn–O distances involving the bridging ligand indicates an essentially symmetric mode of coordination, and the Sn(2)–O(4) distance, 2.190(4) Å, is the shortest of the Sn–O(carboxylate) distances owing to the unidentate mode of coordination of this ligand. There are two relatively close intramolecular contacts of note for structure type A and these are also found in the structure of **2**. The

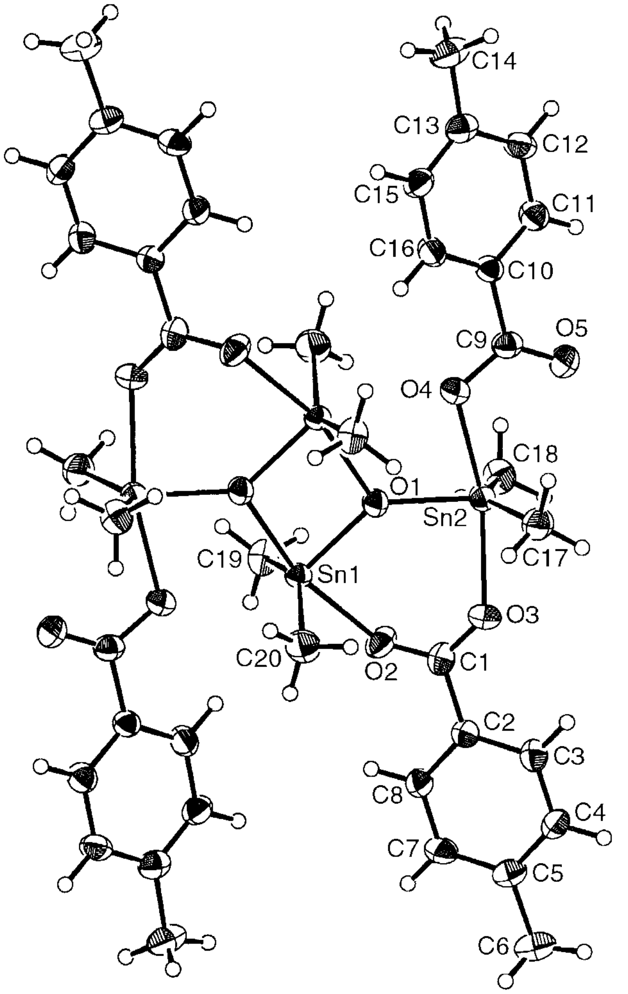

Fig. 4. Molecular structure and crystallographic numbering scheme employed for **2**.

closest of these is the Sn(1)–O(4)′ contact of 2.678(4) Å (related by a centre of inversion) and the other of 2.994(5) Å occurs between the Sn(2) and O(5) atoms. The O(5) atom also forms a weak intermolecular contact of 3.394(5) Å to a symmetry related Sn(2) atom (symmetry operation: $-x$, y, $0.5 - z$). The length of this separation, coupled with the short C(9)–O(5) distance suggests that this interaction is only weak, certainly when compared to the intermolecular separation of 2.56(1) Å in **1**. In the lattice, the tetranuclear clusters stack long the crystallographic *b*-direction with the interplanar separation between aromatic rings being 4.0 Å; the intermolecular Sn···O interactions run parallel to the *c*-axis. It is likely that the oxygen atoms involved in the close Sn···O contacts only influence the coordination geometries rather than being indicative of significant interactions. Thus, the major distortions from the ideal trigonal bipyramidal geometries about both the Sn(1) and Sn(2) atoms, i.e., C–Sn–C, may be traced to the close approach of the respective oxygen atoms.

3.4. Dynamic processes

The broadness of the endo ^{119}Sn resonance is indicative of some dynamic process involving the endocyclic tin atom but not the exocyclic one of **1**, **2** and **3** in solution. This fluxionality is not the one previously invoked [6,40] to account for exchange averaging of the ^{1}H and ^{13}C resonances of the heterotopic carboxylate moieties while those of the heterotopic diorganotin moieties remain duplicated, as is likewise observed here for **1** and **2**.

With the purpose of getting insight into this dynamic process, variable temperature ^{119}Sn NMR spectra were recorded for **1**. Decreasing the temperature down to 203 K maintains a pair of resonances. This indicates that in solution, the structure of **1** does not freeze out to type B (Fig. 1), observed in the solid state. Hence, the nonsymmetric solid state structure [4] is probably due to a crystal packing effect. However, while the chemical shift of the exocyclic tin atom slightly shifts to lower frequency by 2.5 ppm, that of the endocyclic tin atom, unexpectedly, shifts to higher frequency by 5.4 ppm upon cooling. In addition, the associated resonance does not broaden further but rather narrows out, as the temperature is lowered.

These findings are interpreted by a fast equilibrium between type A and type C structures. It is noted that such an equilibrium explains that all carboxylate resonances are averaged out on the ^{1}H and ^{13}C NMR time scales, since the equilibrium between A and C can be considered as half of the dynamic process of A described previously [6], in which mono- and bidentate carboxylates of structure A are exchanged. Because the isotropic ^{119}Sn chemical shift of the endo tin atom in the solid state lies by far at lower frequency in the type C (cf. **3**) than in the type A (cf. **2** and **4**) structure, it must, somewhat unexpectedly, be concluded that the open structure A is favoured at low temperature since a high frequency shift is observed upon cooling. Accordingly, the closed structure C would be favoured at high temperature. It can be seen formally as a cyclodimer of Me_2SnO units complexed by two $(R'COO)_2SnR_2$ units, so that such structure C would be the precursor of the decomposition of bis[dicarboxylatotetraorganodistannoxanes] into two Me_2SnO and two $(R'COO)_2SnR_2$ units. On the other hand, as the high frequency shift upon cooling is quite small and the ^{119}Sn chemical shift is closer to those of structure A in the whole temperature range, there is only a small fraction of the type C structure involved in the dynamic equilibrium of **1** at all temperatures, so that in solution, structure A is obviously favoured thermodynamically.

4. Conclusion

From our parallel investigation on X-ray, 2D ^{1}H–^{119}Sn HMQC and ^{119}Sn MAS NMR data, it clearly appears that ^{119}Sn resonance assignments to endo and exo tin atoms of bis[dicarboxylatotetraorganodistannoxanes] is subject to no fixed rule, a full assignment strategy being obviously needed for both solid and solution states on a case-by-case basis. However, ^{119}Sn MAS NMR spectroscopy appears to be a powerful tool for discriminating between types A, B and C structures. With regards to discrimination between endo and exo tin atoms in type A structures (compounds **2** and **4**), the larger ^{119}Sn chemical shift difference between the endo and exo tin atoms in the solid state as compared to the solution state suggests that the high frequency ^{119}Sn chemical shift can be assigned to the exo tin atom, by comparison with the high ^{119}Sn chemical frequency shifts of **1** and **3**.

Acknowledgements

The financial support of the Belgian Flemish Science Foundation (FKFO, grant nr 2.0094.94) and of the Belgian 'Nationale Loterij' (Grant no. 9.0006.93) is gratefully acknowledged (R.W., M.B.). The authors are indebted to the European Union Program 'Human Capital and Mobility' (R.W., C.S.) for financial support (contract ERBCHRX-CT-94-0610). Research grants from the Australian Research Council (E.R.T.T.) are gratefully acknowledged. A post-doctoral grant of the Flemish 'Fonds voor Wetenschappelijk Onderzoek Vlaanderen' is gratefully acknowledged (A.M.).

References

[1] E.R.T. Tiekink, Appl. Organomet. Chem. 5 (1991) 1.
[2] E.R.T. Tiekink, in: Trends in Organometallic Chemistry, Council of Scientific Research Integration, Trivandrum, India 1994, Vol. 1, p. 71.
[3] M. Gielen, P. Lelieveld, D. de Vos, R. Willem, in: B.K. Keppler (Ed.), Metal Complexes in Cancer Chemotherapy, VCH, Weinheim, 1993, p. 369.
[4] T.P. Lockhart, W.F. Manders, E.M. Holt, J. Am. Chem. Soc. 108 (1986) 6611.
[5] M. Gielen, E.R.T. Tiekink, A. Bouhdid, D. de Vos, M. Biesemans, I. Verbruggen, R. Willem, Appl. Organomet. Chem. 9 (1995) 639.
[6] E.R.T. Tiekink, M. Gielen, A. Bouhdid, M. Biesemans, R. Willem, J. Organomet. Chem. 494 (1995) 247.
[7] M. Gielen, A. Bouhdid, R. Willem, V.I. Bregadze, L.V. Ermanson, E.R.T. Tiekink, J. Organomet. Chem. 501 (1995) 277.
[8] M. Gielen, M. Biesemans, A. El Khloufi, J. Meunier-Piret, F. Kayser, R. Willem, J. Fluorine Chem. 64 (1993) 279.
[9] M. Gielen, A. El Khloufi, M. Biesemans, F. Kayser, R. Willem, Appl. Organomet. Chem. 7 (1993) 201.
[10] M. Gielen, A. El Khloufi, M. Biesemans, R. Willem, Appl. Organomet. Chem. 7 (1993) 119.
[11] T. Yano, K. Nakashima, J. Otera, R. Okawara, Organometallics 4 (1985) 1501.
[12] D. Dakternieks, K. Jurkschat, S. van Dreumel, E.R.T. Tiekink, Inorg. Chem. 36 (1997) 2023.
[13] C. Vatsa, V.K. Jain, T. Kesavadas, E.R.T. Tiekink, J. Organomet Chem. 408 (1991) 157.
[14] J. Bonetti, C. Gondard, R. Pétiaud, M.-F. Llauro, A. Michel, J. Organomet. Chem. 481 (1994) 7.
[15] R. Willem, A. Bouhdid, A. Meddour, C. Camacho-Camacho, F. Mercier, M. Gielen, M. Biesemans, F. Ribot, C. Sanchez, E.R.T. Tiekink, Organometallics 16 (1997) 4377.
[16] J. Mason, Multinuclear NMR, Plenum, New York, 1987, pp. 625–629.
[17] A.G. Davies, P.G. Harrison, J.D. Kennedy, R.J. Puddephatt, T.N. Mitchell, W. McFarlane, J. Chem. Soc. A (1969) 1136.
[18] B. Wrackmeyer, Annu. Rep. NMR Spectrosc. 16 (1985) 73.
[19] J. Keeler, R.T. Clowes, A.L. Davis, E.D. Laue, Meth. Enzymol. 239 (1994) 145.
[20] J.-M. Tyburn, I.M. Bereton, D.M. Doddrell, J. Magn. Reson. 97 (1992) 305.
[21] J. Ruiz-Cabello, G.W. Vuister, C.T.W. Moonen, P. Van Gelderen, J.S. Cohen, P.C.M. Van Zijl, J. Magn. Reson. 100 (1992) 282.
[22] G.W. Vuister, R. Boelens, R. Kaptein, R.E. Hurd, B.K. John, P.C.M. Van Zijl, J. Am. Chem. Soc. 113 (1991) 9688.
[23] A. Bax, R.H. Griffey, B.L. Hawkins, J. Magn. Reson. 55 (1983) 301.
[24] A. Bax, M.F. Summers, J. Am. Chem. Soc. 108 (1986) 2093.
[25] A. Bax, M.F. Summers, J. Magn. Reson. 67 (1986) 565.
[26] F. Kayser, M. Biesemans, M. Gielen, R. Willem, J. Magn. Reson. A 102 (1993) 249.
[27] J.C. Martins, P. Verheyden, F. Kayser, M. Gielen, R. Willem, M. Biesemans, J. Magn. Reson. 124 (1997) 218.
[28] F. Kayser, M. Biesemans, M. Gielen, R. Willem, in: M. Gielen, R. Willem, B. Wrackmeyer (Eds.), Advanced Applications of NMR to Organometallic Chemistry, Wiley, Chichester, 1996, Chap. 3, pp. 45–86.
[29] R. Willem, A. Bouhdid, F. Kayser, A. Delmotte, M. Gielen, J.C. Martins, M. Biesemans, B. Mahieu, E.R.T. Tiekink, Organometallics 15 (1996) 1920.
[30] A. Sebald, in: P. Diehl, E. Fluck, H. Günther, R. Kosfeld, J. Seelig, (Eds.), Solid State NMR II: Inorganic Matter, MAS and CP/MAS NMR of Less Common Spin-1/2 Nuclei, Springer-Verlag, Berlin, 1994, p. 91.
[31] A. Sebald, in: M. Gielen, R. Willem, B. Wrackmeyer (Eds.), Advanced Applications of NMR to Organometallic Chemistry, Wiley, Chichester, 1996, Chap. 5, pp. 123–157.
[32] H. Reuter, A. Sebald, Z. Naturforsch. 48b (1992) 195.
[33] D. Massiot, H. Thiele, A. Germanus, Bruker Rep. 140 (1994) 43.
[34] J. Herzfeld, A.E. Berger, J. Chem. Phys. 73 (1980) 6021.
[35] U. Haeberlen, Adv. Magn. Reson. Suppl. 1 (1976) .
[36] TEXSAN, Structure Analysis Package, Molecular Structure, TX, 1992.
[37] N. Walker, D. Stuart, Acta Crystallogr. Sect. A 39 (1983) 158.
[38] P.T. Beurskens, G. Admiraal, G. Beurskens, W.P. Bosman, S. Garcia-Granda, J.M.M. Smits, C. Smykalla, The DIRDIF program system, Technical Report of the Crystallography Laboratory, University of Nijmegen, The Netherlands, 1992.
[39] C.K. Johnson, ORTEP-II, Report ORNL-5138, Oak Ridge National Laboratory, Oak Ridge, TN, 1976.
[40] D.C. Gross, Inorg. Chem. 28 (1989) 2355.
[41] T.P. Lockhart, W.F. Manders, J.J. Zuckerman, J. Am. Chem. Soc. 107 (1985) 4546.

[42] R.K. Harris, S.E. Lawrence, S.W. Oh, V.G. Kumar Das, J. Mol. Struct. 347 (1995) 309.
[43] R.K. Harris, J.D. Kennedy, W. McFarlane, in: NMR and Periodic Table, Academic Press, London, 1978, p. 348.
[44] M. Gielen, A. Bouhdid, F. Kayser, M. Biesemans, D. de Vos, B. Mahieu, R. Willem, Appl. Organomet. Chem. 9 (1995) 251.
[45] M. Gielen, M. Biesemans, A. El Khloufi, J. Meunier-Piret, F. Kayser, R. Willem, J. Fluorine Chem. 64 (1993) 279.
[46] M. Gielen, A. Bouhdid, E.R.T. Tiekink, Main Group Met. Chem. 18 (1995) 199.
[47] C. Vatsa, V.K. Jain, T. Kesavadas, E.R.T. Tiekink, J. Organomet. Chem. 410 (1991) 135.
[48] S. Narula, S.K. Bharadwaj, Y. Sharda, R.O. Day, L. Howe, R.R. Holmes, Organometallics 11 (1992) 2206.
[49] A. Meriem, R. Willem, J. Meunier-Piret, B. Mahieu, M. Gielen, Main Group Met. Chem. 13 (1990) 167.
[50] M. Gielen, M. Bouâlam, B. Mahieu, R.T. Tiekink, Appl. Organomet. Chem. 8 (1994) 19.
[51] E. Klaus, A. Sebald, Magn. Reson. Chem. 32 (1994) 679.